

Augmented interferon regulatory factor 7 axis in whole tumor cell vaccines prevents tumor recurrence by inducing interferon gamma-secreting B cells

Nabeel Kajihara^a, Yoshino Tanaka^a, Riko Takeuchi^a, Takuto Kobayashi^a, Masafumi Tanji^a, Tsukasa Ataka^a, Shiho Nakano^a, Taisho Yamada^b, Akinori Takaoka^b, Yoshinori Hasegawa^c, Ken-Ichiro Seino^{a#}, and Haruka Wada^{a#}

^aDivision of Immunobiology, Graduate School of Medicine, Institute for Genetic Medicine, Hokkaido University, Sapporo, Japan; ^bDivision of Signaling in Cancer and Immunology, Institute for Genetic Medicine, Hokkaido University, Sapporo, Japan; ^cLaboratory of Gene Sequencing Analysis, Department of Applied Genomics, Kazusa DNA Research Institute, Kisarazu, Japan

ABSTRACT

Among cancer immunotherapy, which has received great attention in recent years, cancer vaccines can potentially prevent recurrent tumors by using the exquisite power and specificity of the immune system. Specifically, whole tumor cell vaccines (WTCVs) based on surgically resected tumors have been considered to elicit robust anti-tumor immune responses by exposing various tumor-associated antigens to host immunity. However, most tumors have little immunogenicity because of immunoediting by continuous interactions with host immunity; thus, preparing WTCVs based on patient-derived non-modified tumors cannot prevent tumor onset. Hence, the immunogenicity of tumor cells must be improved for effective WTCVs. In this study, we indicate the importance of the interferon regulatory factor 7 (Irf7) axis, including Irf7 and its downstream factors, within tumor cells in regulating immunogenicity. Indeed, WTCVs that augmented the Irf7 axis have exerted remarkable recurrence-preventive effects when vaccinated after tumor inactivation by radiation. Most notably, vaccination with murine colon cancer cells that enhanced the Irf7 axis prevented the development of challenged tumors in all mice and resulted in a 100% survival rate during the observation period. Furthermore, the mechanism leading to vaccine effectiveness was mediated by interferon-gamma-producing B cells. This study provides novel insights into how to enhance tumor immunogenicity and use WTCVs as recurrence prophylaxis.

ARTICLE HISTORY

Received 4 February 2023

Revised 17 April 2023

Accepted 8 May 2023

KEYWORDS

B cell; IFN γ ; Irf7; vaccine; whole tumor cell vaccine

Introduction

With medical advances in cancer treatment, even though some patients achieve complete remission through standard treatments, such as surgical resection, chemotherapy, and radiation therapy, numerous tumor cases recur later, because these treatments may fail to eliminate residual and micro-metastatic tumor cells¹. Cancer immunotherapy, which has received considerable attention as the fourth cancer treatment option in recent years, exploits the exquisite power and specificity of the immune system to boost the host's natural immune response to cancer, not only to eradicate malignancy, but also to significantly reduce future cancer recurrence risk².


Among cancer immunotherapy, cancer vaccines specifically aim to destroy cancer cells by establishing an active tumor-specific T-cell population against tumor-specific antigens distinct from self-antigens³. Cancer vaccines are classified as cell-based, protein-/peptide-based, or gene-based vaccines⁴. Although manufacturing protein-/peptide-based and gene-based vaccines must determine the best tumor-specific antigen candidate, it is not required for producing cell-based vaccines⁵. Cell-based vaccines include whole tumor cells, tumor cell lysates, or dendritic cells to which tumor-associated antigens (TAAs) are

loaded, and they have been manufactured generally from patient-derived autologous cells². The best-known cell-based vaccine is Sipuleucel-T, one of the dendritic cell vaccines, and it has been approved for clinical use in the treatment of advanced prostate cancer in the United States⁶. However, this strategy improved overall survival by only 4 months in the clinical trial because⁷: controlling transferred-dendritic cells to migrate to lymph nodes and interact with T cells is challenging, and the variety of TAAs that can be loaded is limited by the number of transferred-dendritic cells. Eventually, the approval was withdrawn because of commercial and cost-effectiveness concerns.

By contrast, whole tumor cell vaccines (WTCVs) from patients contain diverse TAAs; theoretically, they can elicit a broad-spectrum anti-tumor immune response when inoculated in the body³. Nevertheless, clinical trials using melanoma tumors have limited results because an objective clinical response was observed in <10% of cases⁸. One reason for this unfortunate outcome is that most tumors, the source of WTCVs, lack inherently potent immunogenicity because of cancer immunoediting. Tumor cells evolve during the continuous interaction with the host immune system and, troublingly, can eventually escape from immune surveillance⁹.

CONTACT Ken-ichiro Seino  seino@igm.hokudai.ac.jp; Haruka Wada  wada@igm.hokudai.ac.jp  Division of Immunobiology, Graduate School of Medicine, Institute for Genetic Medicine, Hokkaido University, Kita-15 Nishi-7, Sapporo 060-0815, Japan

#Haruka Wada and Ken-ichiro Seino contributed equally to this work.

 Supplemental data for this article can be accessed online at <https://doi.org/10.1080/2162402X.2023.2213132>.

© 2023 The Author(s). Published with license by Taylor & Francis Group, LLC.

This is an Open Access article distributed under the terms of the Creative Commons Attribution-NonCommercial License (<http://creativecommons.org/licenses/by-nc/4.0/>), which permits unrestricted non-commercial use, distribution, and reproduction in any medium, provided the original work is properly cited. The terms on which this article has been published allow the posting of the Accepted Manuscript in a repository by the author(s) or with their consent.

Therefore, the immunogenicity of tumor cells must be improved to succeed in this therapeutic approach.

Accumulating evidence shows that immunogenic cell death is promoted in dying tumor cells because of the release of intracellular immunogenic antigens caused by cancer treatments, such as chemotherapy and radiotherapy¹⁰. Indeed, previous data, including our results, indicate that irradiating tumor cells promotes high vaccine effectiveness in WTCVs using several cancer cell lines. Conversely, some cancer cell lines represented no or little tumor suppression even when vaccinated after radiation¹¹. To overcome these issues, recent studies have reported that immunogenicity can be enhanced, and anti-tumor immune responses can be induced by genetically modifying tumor cells to express immunostimulatory molecules or secrete cytokines¹.

One strategy is to use genetically modified tumor cells to secrete granulocyte-macrophage colony-stimulating factor (GM-CSF). Many studies in murine tumor models have demonstrated that WTCVs by GM-CSF transgenic tumor cells induce potent systemic immunity¹². Moreover, although this method is still not clinically used, it showed encouraging clinical outcomes in some clinical trials¹³. It has been attributed to the role of GM-CSF in differentiating and activating dendritic cells at the vaccination site¹³. Another strategy is to enhance the tumor cells' immunogenicity, and studies have considered that antiviral responses elicited by interferon (IFN) are also serviceable^{14,15}. Augmenting the IFN pathway is one of the most crucial immunogenic triggers of all aspects of innate and adaptive immunity¹⁶; in fact, the transduction of type I or II IFNs into tumor cells has been confirmed to enhance the efficacy of cancer vaccines in specific cancer^{14,15}.

Despite research on cancer vaccines, no current approach has been clinically indicated as WTCVs. Therefore, basic research regarding cancer vaccines is significant and provides an excellent opportunity to explore a clinically beneficial method. In this study, we aimed to investigate the potential of new cancer vaccine therapies by identifying some IFN-related factors, such as gene characteristics of cancer cells with high vaccine effectiveness, and introducing them into cancer cells with low vaccine effectiveness. This study will give some hints about the future development of cancer vaccines.

Materials and methods

Cell lines

Mouse breast cancer cell line 4T1, mouse colon cancer cell line CT26, mouse lung cancer cell line 3LL, mouse melanoma cell line B16, and mouse fibrosarcoma cell line MCA205 were purchased from the American Type Culture Collection. 4T1 was designated as 4T1-ATCC (4T1A) and the highly immunogenic sub-clone of 4T1A, established in 2015, was named 4T1-Sapporo (4T1S)¹¹. All cell lines were maintained in RPMI-1640 (Fujifilm Wako Pure Chemical Corporation). Culture medium was supplemented with 10% fetal bovine serum (FBS) (Sigma-Aldrich), 100 U/ml penicillin (Nacalai Tesque), 100 µg/ml streptomycin (Nacalai Tesque), 0.1 mM MEM nonessential amino acids (Nacalai Tesque), and maintained at 37°C with 5%

CO₂. Mycoplasma contamination of cell lines was checked using the MycoAlert® Mycoplasma Detection Kit (Lonza Group), according to the manufacturer's instructions; no contamination was found.

Generation of transfected cell lines and *Irf7* knockout (KO) cell line

The coding sequences of the candidate genes (*Irf7*, *Ifi44*, *Usp18*, and *Oas3*) were synthesized using 4T1S cDNA as a template and subcloned into the pPyCAG vector (kindly provided by Dr. Niwa, RIKEN). The *Irf7* double nickase plasmid (Santa Cruz Biotechnology) was used to generate the *Irf7*KO cell line. *Irf7*-expressing, *Ifi44*-expressing, *Usp18*-expressing, *Oas3*-expressing, and *Irf7* double nickase plasmids were transfected into 2×10^6 tumor cells using the Neon® transfection system (Thermo Fisher Scientific), and cells were incubated for 24 h for curing. The efficiency of transfection of *Irf7* double nickase plasmid into cells was checked by expression of green fluorescent protein (GFP), and all GFP-positive cells were sorted by FACSaria™ II (BD Biosciences). Then, puromycin (6 µg/ml) was added to the medium, and transfected cells were selected by incubation for 96 h. The expression of the KO gene (*Irf7*) in these cells was examined by western blotting, and we used the cells in bulk for experiments. Since the expressing plasmids of *Irf7*, *Ifi44*, *Usp18*, and *Oas3* do not contain a GFP reporter gene, transgenic cells were selected by adding puromycin (2 ~ 10 µg/ml) to the medium and cultured for 96 h. The expression of each transgene (*Irf7*, *Ifi44*, *Usp18*, and *Oas3*) was examined by RT-PCR, and we used the cells in bulk for experiments.

Mouse in vivo experiments

Six to seven weeks old female BALB/c, BALB/c *nu/nu*, and C57BL/6 mice were purchased from Japan SLC. The mice were maintained under specific pathogen-free conditions and housed in 12-h light/12-h dark cycle in the animal facility at Hokkaido University. For in vivo prophylactic vaccination assay, 2×10^6 tumor cells were resuspended in 200 µl PBS and inoculated subcutaneously into the right back of syngeneic female mice after 300 Gray X-rays as WTCVs. Two weeks after vaccination, 5×10^4 tumor cells (without radiation) were resuspended in 200 µl PBS and inoculated subcutaneously into the left mammary gland as a challenging tumor. The day a palpable tumor could be confirmed was defined as tumor onset day in the Kaplan–Meier plot. Anti-CD20 antibodies (250 µg, #152104, BioLegend) were intraperitoneally administered seven days before, 1 day before, and 7 days after vaccination. If tumor-free or survival was prolonged till day 100 after the tumor challenge, observation was terminated the day. In the experiments examining immune cells in lymph nodes, axillary and inguinal lymph nodes were isolated after mice were sacrificed. For in vivo therapeutic vaccination assay, 1×10^5 tumor cells were resuspended in 10 µl PBS and inoculated subcutaneously into the right flank of syngeneic female mice. Five days and ten days post-tumor inoculation, 2×10^6 tumor cells after 300 Gray X-rays were inoculated subcutaneously into the right back. Tumor size was measured by a caliper three

times a week and observed until day 14. The Animal Care Committee of Hokkaido University approved all animal experiments (Approval number: 22–0138).

Gene expression analysis

Gene expression was analyzed by reverse transcription-polymerase chain reaction (RT-PCR). Total RNA was extracted using TRIsure reagent (NIPPON Genetics). cDNA was synthesized from extracted RNA using ReverTra Ace[®] qPCR RT Master Mix (TOYOBO). PCR was performed on cDNA using KAPA SYBR[®] FAST qPCR Kit Master Mix (2×) ABI Prism[™] (NIPPON Genetics) on a StepOnePlus Real-Time PCR System (Thermo Fisher Scientific). Glyceraldehyde-3-phosphate dehydrogenase gene (*Gapdh*) expression was used as internal control, and the expression levels of each target gene were normalized to *Gapdh*. The corresponding primers were as follows:

Gapdh: Fw-TCAAATGGGGTGAGGCCGGT, Rv-TTGCTGACAATCTTGAGTGA

Irf7: Fw-TCCTGAGCGCAGCCTTG, Rv-GTTCCTACTGCTGGGGCCAT

Ifi44: Fw-TACACACGTGGATAGCCTGGA, Rv-CTTCAGTGCCGAGAGGATCA

Usp18: Fw-CAGGAGTCCCTGATTTGCGT, Rv-GGGCTGGACGAAACATCTCA

Oas3: Fw-CCTGATCCGGCTGGTGAAAT, Rv-CCCAGGCGTACACAGTTAGG

Ifna: Fw-ATGGCTAGCTCTGTGCTTTCT, Rv-AGGGCTCTCCAGATTCTGCTCTG

Ifnb: Fw-ATCAACCTCACCTACAGGGC, Rv-ATCTCTTGATGGCAAAGGCA
Ifng: Fw-AAGACAATCAGGCCATCAGCA, Rv-AGCGACTCCTTTCCGCTT

Protein expression analysis

Protein expression analysis for *Irf7* in 4T1A, 4T1S, and *Irf7KO* 4T1S cell lines was performed by western blotting. To also examine radiation-induced changes in *Irf7* expression levels, the cells were irradiated with 300 Gray X-rays and collected 24 hours later. Cell lysates were obtained from each cell line by lysing in RIPA buffer (150 mM NaCl, 50 mM Tris-HCl, 0.5% deoxycholic acid sodium salt, 1% triton, 0.1% sodium dodecyl sulfate (SDS)) containing 100 μM phenylmethylsulfonyl fluoride (PMSF) and disrupted by Bioruptor UCD-250 (Sonicbio), followed by centrifuged to collect a supernatant sample. Then, we added a 4×SDS sample buffer (0.25 M Tris-HCl, 8% SDS, 20% glycerol, 0.02% bromophenol blue, 20% 2-mercaptoethanol) to each supernatant sample and stored at −20°C. Before use, we boiled the samples at 100°C. Protein was separated by electrophoretic migration at 200 V using a 15% acrylamide gel and transferred to a polyvinylidene difluoride membrane at 100 V. The membrane was blocked with 5% skim milk in TBS-T (138 mM NaCl, 2.7 mM KCl, 50 mM tris, 0.05% tween20) at 4°C overnight, then probed with 1:1000 dilution of anti-*Irf7*

antibodies (#72073S, Cell Signaling Technology) at room temperature for 1 h with gentle shaking, followed by incubation in 1:3000 dilution of horseradish peroxidase-conjugated anti-rabbit IgG antibodies (#7074S, Cell Signaling Technology) at room temperature for 30 min with gentle shaking. Proteins were visualized (exposure time: 500 s) using Super Signal West Femto Maximum Sensitivity Substrate (#34095, Thermo Fisher Scientific). The bands were quantified using ImageJ. As an internal control molecule, we detected Tubulin with a 1:3000 dilution of anti-α Tubulin antibodies (#sc -23,948, Santa Cruz Biotechnology).

Single-cell RNA sequencing

Lymph nodes from each mouse were collected 14 days after vaccination with 4T1A or 4T1S. Isolated lymph node cells were prepared as libraries from cell suspension according to the BD Rhapsody[™] Express Single-Cell Analysis System Instrument User Guide. Briefly, cells were lysed, cDNA was synthesized using the BD Rhapsody[™] WTA Amplification Kit (BD Biosciences), and library preparation was performed using the BD Rhapsody[™] Library Preparation Kit (BD Biosciences) following the manufacturer's protocol. The amplified cDNA was fragmented and tagged with unique molecular identifiers (UMIs) using the BD Rhapsody[™] Tagging Kit (BD Biosciences). The tagged fragments were amplified, purified, and sequenced on the MGI Tech DNBSEQ G400RS system performing paired-end 100 base pair reads at Kazusa DNA Research Institute, Japan. The raw sequencing data were processed using the BD Rhapsody[™] Analysis Pipeline (BD Biosciences) to generate gene expression matrices for each cell. The resulting count matrices were further processed using the R package Seurat (v4.0.1) to filter out low-quality cells with fewer than 200 genes detected and to remove mitochondrial and ribosomal RNA reads. Normalization, scaling, and variable gene selection were performed using the SCTransform function in Seurat, and principal component analysis (PCA) was performed on the resulting gene expression matrices. Then, t-distributed stochastic neighbor embedding (tSNE) projections allowed us to assign cells to 12 clusters. Cell types were annotated using the Louvain algorithm based on known cell markers and differential gene expression analysis. Results were visualized using R (v4.0.1) and the following packages: Seurat, ggplot2, and dplyr. We identified highly expressed genes in *CD4*, *CD8a*, and *CD19* clusters within 4T1S vaccinated murine lymph node cells by mean expression and variance compared to 4T1A vaccinated murine lymph node cells and were visualized using the Volcano plots.

Gene ontology enrichment analysis

The differential expression genes (highly expressed genes in each immune cell within lymph nodes of mice vaccinated with 4T1S) for each cluster obtained from the above were imported into the ShinyGO 0.76.2 bioinformatics graphical web application (<http://bioinformatics.sdstate.edu/go/>), and gene ontology analysis of biological processes was performed. The top 10 with higher gene enrichment scores in lymph node *CD4*, *CD8a*, and *CD19* clusters of mice vaccinated with 4T1S were shown.

Figure 4d and S4b, d represent upregulated pathways in cells of 4T1S vaccinated mice.

Analysis of immune cell populations in spleen and lymph nodes

Immune cells within lymph nodes and spleen were analyzed by flow cytometry. Extracellular molecules were stained before intracellular staining. Cells were washed and blocked with FcR Blocking Reagent (BioLegend) and stained with 4', 6-diamidino-2-phenylindole (Cayman Chemical Company) and the antibodies against the following molecules; CD3 ϵ , CD11b, CD11c, CD19, CD20, CD45, F4/80, and Ly6G (BioLegend). After extracellular staining, cells were fixed and permeabilized with Cytotfix/Cytoperm™ Buffer (BD Biosciences), then intracellular IFN γ was stained (BioLegend). Data were acquired using FACSCelesta flow cytometer (BD Biosciences) and analyzed using FlowJo software (BD Biosciences). The gating strategies were as follows; first selected live cells based on forward- and side-scatters, with subsequent selection of singlets. When analyzing immune cells, CD45⁺ cells were gated, then a target population was expanded.

Statistical analysis

Sample size and statistical tests are described in the figure legends. Every series of data are shown as mean \pm SEM. A two-sided Student's *t*-test was used to compare the two groups. One-way ANOVA with the Tukey–Kramer test was used to compare three or more groups. The survival curves of vaccinated mice were determined using the Kaplan–Meier method, and the Log-rank test was used for statistical evaluation. The *P*-value of <0.05 was considered to be statistically significant. All statistical analyses were performed with JMP® Pro 16 software (SAS Institute).

Results

Highly immunogenic tumors express high levels of innate immune-related genes following radiation, resulting in tumor suppression at recurrence

The irradiation of cancer cells as a pretreatment for cancer vaccines is considered promising¹⁷. The irradiation of cancer cells before vaccination cannot only inactivate the proliferative capacity of cancer cells but can also elicit immunogenic death of cancer cells by directly or indirectly damaging their DNA¹⁸. Indeed, preclinical and clinical studies have shown that radiation plays a role in vaccine augmentation^{19,20}. However, the extent of vaccine efficacy differs by cancer types and characteristics, and factors that regulate the efficacy and the detailed mechanisms have not been clarified.

To address this issue, we used six murine cancer cell lines and examined the effectiveness of each vaccine as WTCVs after cancer cell irradiation by immunizing them 2 weeks before the tumor challenge that assumed recurrence. In this study, based on our paper published in 2015, we referred to 4T1 available from ATCC as 4T1A and the highly immunogenic subclone of

4T1, which was established in Sapporo, Japan, as 4T1S¹¹. Certainly, remarkable differences in vaccine effectiveness were observed in each irradiated cancer cell line. In other words, vaccination with irradiated 4T1A, 3LL, and B16 did not intercept challenged tumor development (Figure 1a), whereas irradiated 4T1S, CT26, and MCA205 showed significant tumor suppression compared with the control group (Figure 1b). Based on this result, we hypothesized that a factor with a tumor growth-suppressing effect was highly expressed in cancer cells and influenced the vaccine effectiveness of cancer cells; hence, we investigated gene expression of each cancer cell line after the irradiation. In order of high expression level, four innate immune-related genes, namely, *Irf7*, *IFN-induced protein 44 (Ifi44)*, *ubiquitin-specific peptidase 18 (Usp18)*, and *2'-5'-oligoadenylate synthetase 3 (Oas3)*, were extracted in vaccine-effective cancer cells compared to cancer cells with no vaccine effectiveness (Table 1). Although these extracted factors play significant roles in regulating IFNs induced during the immune response to viral infection^{21,22}, interestingly, no difference was found in the expression of any IFN, including types I – III, between cancer cells with or without vaccine effectiveness (Table 2). These results suggest the possibility that *Irf7*, *Ifi44*, *Usp18*, and *Oas3* in cancer cells contribute to their vaccine effectiveness in an IFN production-independent manner, resulting in recurrence prevention when used as WTCVs.

WTCVs of *Irf7/Ifi44/Usp18* transfected cancer cells afford a better recurrence-preventive effect

To assess the importance of the four candidate factors with respect to their tumor-suppression efficacy as WTCVs, we first established the transfected cancer cell line with *Irf7*, which was the most highly expressed in cancer cells with vaccine effectiveness, into 4T1A without vaccine effectiveness. The expression of *Irf7* in an established cancer cell line was confirmed in ribonucleic acid (RNA) and protein levels (Figure S1a, b). Mice subcutaneously immunized with irradiated *Irf7* transgenic 4T1A and then challenged with naive tumors 2 weeks later were observed to have delayed tumor development and prolonged survival when compared with a control group vaccinated with the 4T1A transfected with the empty vector (Figure 2a). Furthermore, we established the *Irf7* transfected cell line using CT26, which already showed moderate vaccine effectiveness (Figure S1c, d), and their ability was evaluated. Similar results were obtained in the vaccination assay (Figure 2b). These data indicate the value of *Irf7* in vaccine effectiveness by WTCVs.

To achieve a better tumor-suppression rate, a transfected 4T1A that expressed *Ifi44*, the second most highly expressed gene in vaccine-effective cancer cells, was established, in addition to *Irf7* (Figure S1e). Although WTCVs using this cell line also showed tumor suppression and survival extension (Figure 2c), they did not appear to further enhance vaccine effectiveness by *Irf7* alone in transgenic tumors.

Moreover, *Usp18*, the third most highly expressed gene in cancer cells with vaccine effectiveness, was transfected into *Irf7* and *Ifi44* transgenic 4T1A (Figure S1f). To determine

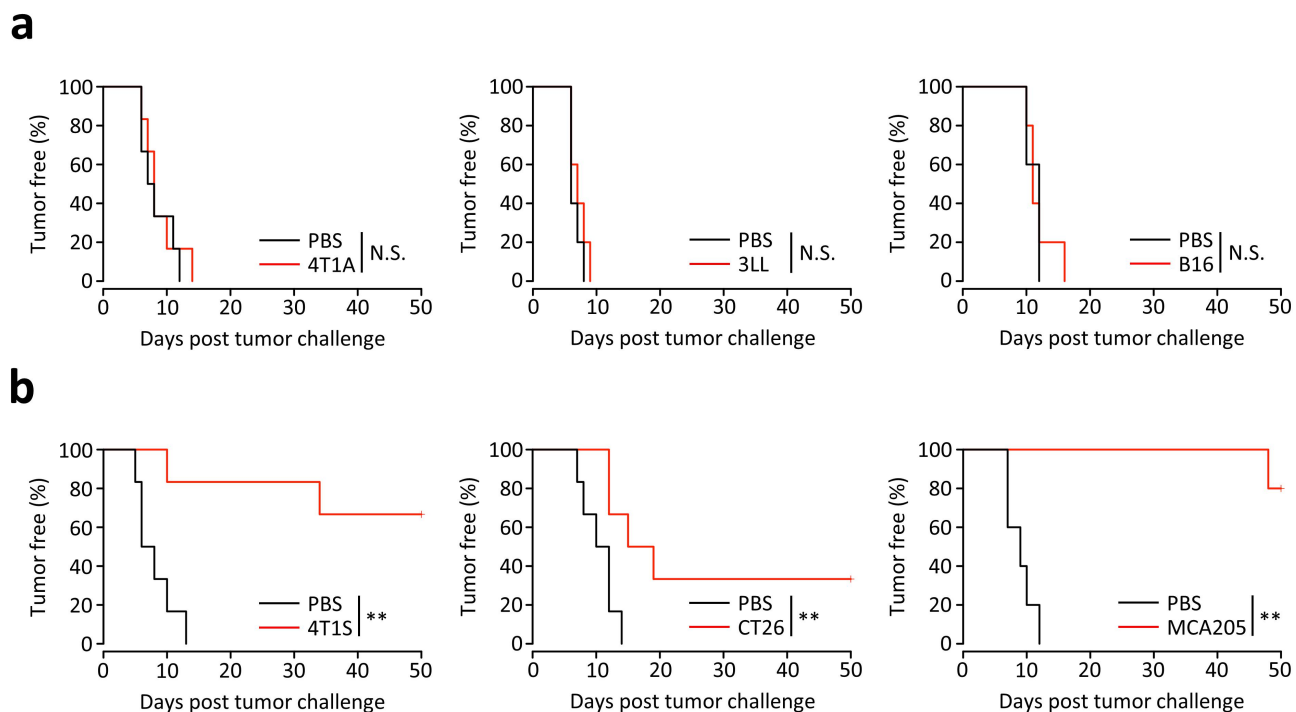


Figure 1. Differences in vaccine effectiveness by irradiated whole tumor cells. Each tumor cell (2×10^6 cells) was resuspended in PBS (200 μ l) and inoculated subcutaneously into the right back of syngeneic female mice after X-rays (300 Gray). Two weeks after vaccination, each tumor cell (5×10^4 cells) of the same type as at the time of vaccination was resuspended in PBS (200 μ l) and inoculated subcutaneously into the left mammary gland. The day a palpable tumor could be confirmed was defined as tumor onset day in the Kaplan–Meier plot. (a, b) Kaplan–Meier plot of tumor-free in BALB/c or C57BL/6 mice vaccinated with 4T1A (n = 6), 3LL (n = 5), B16 (n = 5), 4T1S (n = 6), CT26 (n = 6), or MCA205 (n = 5) cells after radiation. Mice were challenged with 4T1A, 3LL, B16, 4T1S, CT26, or MCA205 cells 2 weeks after the vaccination, respectively. Values were analyzed by a Log-rank test. Asterisk indicates a significant difference; ** $P < 0.01$, compared with the control group.

Table 1. Highly expressed genes in vaccine-effective cancer cells after radiation.

	Gene	B16	4T1A	3LL	CT26	4T1S	MCA205
1	<i>Irf7</i>	0.728359	10.8379	0.802327	74.6452	171.426	179.428
2	<i>Irf44</i>	0.0573365	5.71249	0.229391	40.3954	121.101	84.4698
3	<i>Usp18</i>	1.47266	2.61571	0.709883	49.4265	102.497	29.8158
4	<i>Oas3</i>	0.0431175	3.82767	1.21418	26.4166	50.2315	28.879

A list of genes that showed 5-fold or greater gene expression levels in all combinations from vaccine-ineffective to vaccine-effective cancer cells, with fragments per kilobase of exon per million reads mapped (FPKM) values of 20 or greater in all vaccine-effective cancer cells. The genes are arranged in order of high gene expression level in vaccine-effective cancer cells.

Table 2. Interferon family gene expression in each radiated cancer cell.

Gene	B16	4T1A	3LL	CT26	4T1S	MCA205
<i>Irfn1</i>	0	0.119172	0	0	0	0.055595
<i>Irfn2</i>	0	0	0	0.11328	0	0
<i>Irfn4</i>	0	0	0	0	0.194503	0
<i>Irfn5</i>	0	0	0	0	0	0.055595
<i>Irfn6</i>	0	0	0	0	0	0
<i>Irfn7</i>	0.0976421	0	0	0	0	0
<i>Irfn9</i>	0	0	0	0	0	0
<i>Irfn11</i>	0	0	0	0	0	0
<i>Irfn12</i>	0	0	0	0	0	0
<i>Irfn13</i>	0	0	0	0	0.0708513	0
<i>Irfn14</i>	0	0	0	0	0	0
<i>Irfnb</i>	0	0	0	0	0	0
<i>Irfnb1</i>	0.0658191	0	0	0.529973	2.99051	0.0737542
<i>Irfng</i>	0.0379548	0	0.022282	0	0	0.042493
<i>Irfne</i>	0	0.0961778	0	0	0	0.0897744
<i>Irfnk</i>	0	0	0	0	0	0
<i>Irfnz</i>	0.259398	0.0367919	0.165214	0.247496	0.06106	0.104543

whether vaccination with *Irf7/Irf44/Usp18* transgenic 4T1A protects mice against the growth of recurrent tumors, they were administered to BALB/c mice. Two weeks following the vaccination, when mice were challenged with naive tumors,

mice vaccinated with transgenic tumors presented drastic suppression effects of tumor onset; some mice remained tumor-free for 100 days after the tumor challenge (Figure 2d). Most notably, the WTCV by CT26 transfected

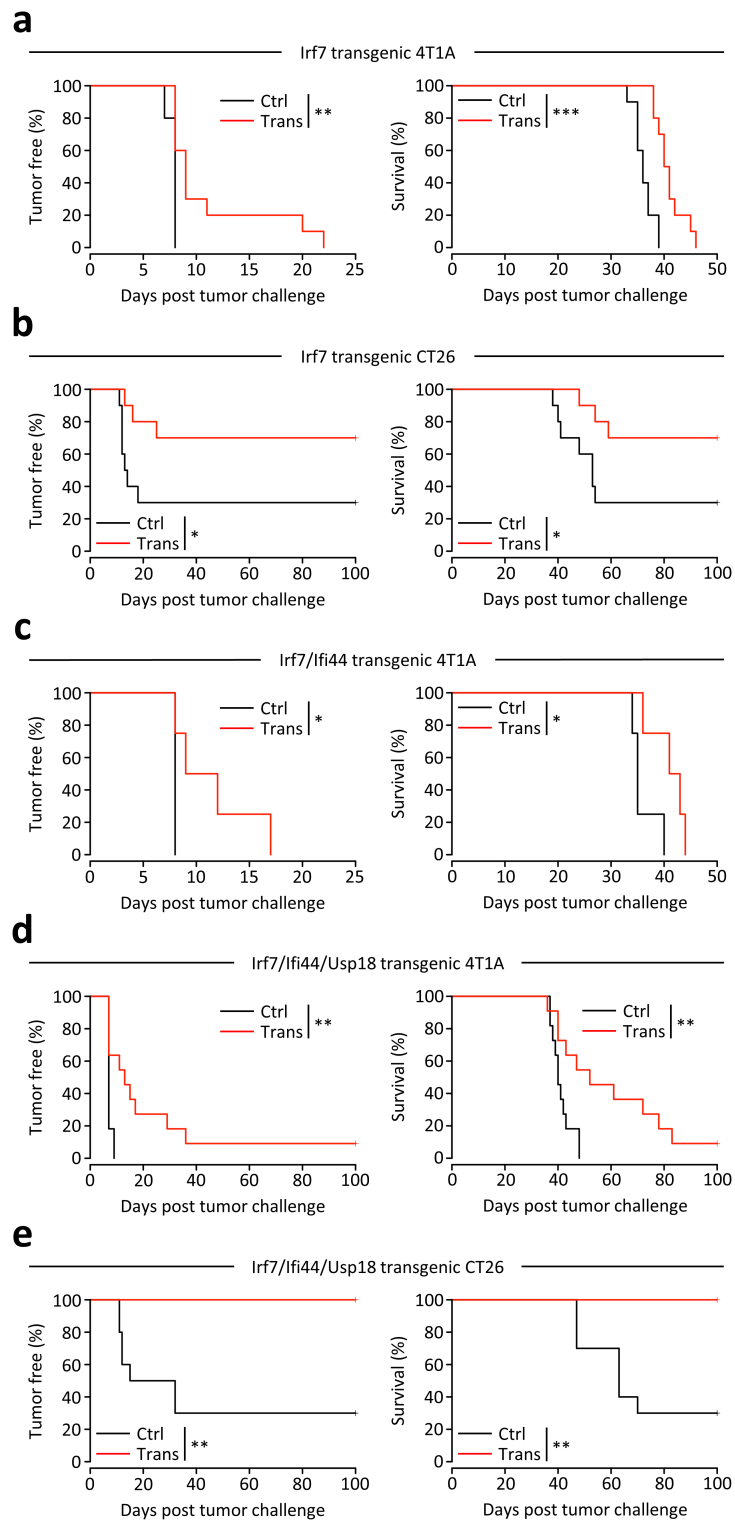


Figure 2. Vaccine effectiveness by each irradiated transgenic whole tumor cell. Each tumor cell (2×10^6 cells) was resuspended in PBS (200 μ l) and inoculated subcutaneously into the right back of syngeneic female mice after X-rays (300 Gray). Two weeks after vaccination, each wild-type tumor cell (5×10^4 cells) was resuspended in PBS (200 μ l) and inoculated subcutaneously into the left mammary gland. The day a palpable tumor could be confirmed was defined as tumor onset day in the Kaplan–Meier plot. (a–e) Kaplan–Meier plot of tumor-free and overall survival in BALB/c mice vaccinated with *lrf7* transgenic 4T1A ($n = 10$) or CT26 ($n = 10$), *lrf7/Ifi44* transgenic 4T1A ($n = 4$), and *lrf7/Ifi44/Usp18* transgenic 4T1A ($n = 11$) or CT26 ($n = 10$) cells after radiation. Mice were challenged with each wild-type cell 14 days after the vaccination. Values were analyzed by a Log-rank test. Asterisk indicates a significant difference; * $P < 0.05$, ** $P < 0.01$, *** $P < 0.001$, compared with the control group.

with three genes *lrf7/Ifi44/Usp18* completely suppressed tumor development and led to 100% survival (Figure S1g, 2e). Similarly, the transfection of the three genes into 3LL cells without vaccine effectiveness resulted in a significant

improvement in tumor-suppression efficacy (Figure S1h, i). Incidentally, *lrf7/Ifi44/Usp18* transgenic 4T1A showed no beneficial therapeutic effect as a therapeutic vaccine (Figure S1j).

Although extremely favorable results were obtained in CT26 as described above, only unsatisfactory results, that is, 100% tumor suppression has not been achieved yet, have been obtained with 4T1A. Therefore, to achieve greater vaccine effectiveness in 4T1A, *Oas3*, the fourth most highly expressed gene in vaccine-effective cancer cells after *Irf7*, *Ifi44*, and *Usp18*, was also introduced (Figure S2a). Interestingly, the hitherto benefit of gene transfer to cancer cells on vaccine efficacy was canceled by the transfection of *Oas3* (Figure S2b). These observations suggest that the anti-tumor effect generated by vaccine-effective cancer cells, such as 4T1S, relies on not *Oas3* but *Irf7*, *Ifi44*, and *Usp18*. By contrast, cancer cells without vaccine effectiveness may have shown poor outcomes because of too little or the lack of their expression.

Irf7 serves as an upstream factor regulating the effects of WTCVs

Given the close operation of *Irf7*, *Ifi44*, and *Usp18* in innate immune responses, we then examined which factor is upstream in these genes for the induction of vaccine effectiveness. In the preparation of each *Irf7*, *Ifi44*, or *Usp18* single transgenic 4T1A and analysis of each gene expression, the expression of the

respective transgene in each established transgenic cell line was confirmed. Specifically, *Irf7* transgenic 4T1A did not express only *Irf7* but also *Ifi44* and *Usp18* (Figure 3a), and similar results were also observed in *Irf7* transgenic CT26 (Figure 3b). These findings indicate that *Irf7* is upstream of three genes, namely, *Irf7*, *Ifi44*, and *Usp18*.

To further consolidate the view that *Irf7* is crucial in vaccine effectiveness, the *Irf7*-deficient line (hereafter referred to as knockout [KO]) was generated in 4T1S, which has vaccine effectiveness (Figure 3c). *Irf7* deficiency nullified the tumor protection efficacy by 4T1S, and >80% of the mice immunized with KO developed tumors at the challenge site within 25 days (Figure 3d). The above results collectively demonstrate that *Irf7* is crucial for generating the anti-tumor effect provided by WTCVs.

WTCVs with high immunogenicity enhance B cell-derived IFN γ expression, enhancing the anti-tumor effect

To understand how *Irf7* in cancer cells enhances the anti-tumor effect of WTCVs, irradiated 4T1A with almost no *Irf7* expression and irradiated 4T1S with high *Irf7* expression were administered in mice, and each immune cell population in the

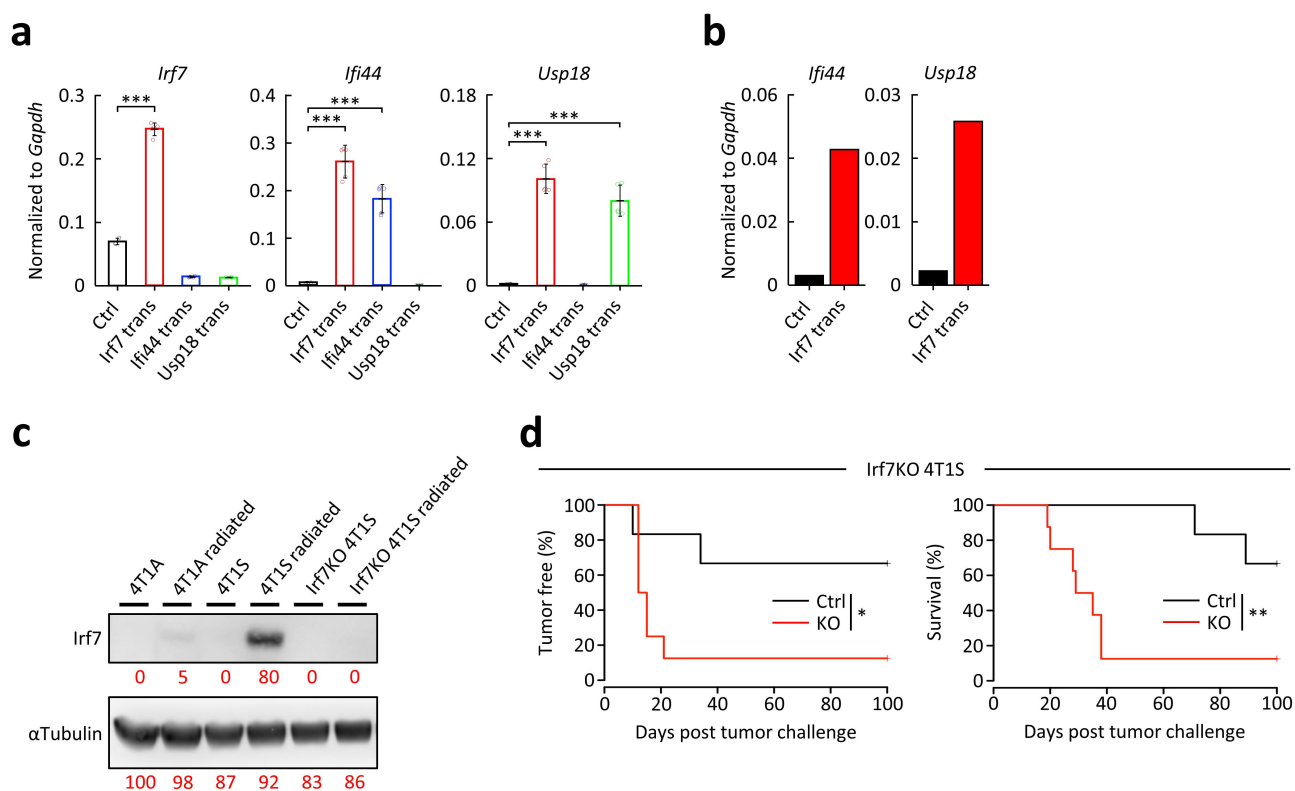


Figure 3. Effects of *Irf7* on vaccine effectiveness by radiated whole tumor cells. *Irf7*-, *Ifi44*-, or *Usp18*-transgenic cells were generated by transfecting *Irf7*-, *Ifi44*-, or *Usp18*-expressing plasmid into tumor cells. *Irf7*KO cell line was generated by transfecting *Irf7* double nickase plasmid into tumor cells. For in vivo prophylactic vaccination assay, each tumor cell (2×10^6 cells) was resuspended in PBS (200 μ l) and inoculated subcutaneously into the right back of syngeneic female mice after X-rays (300 Gray). Two weeks after vaccination, wild-type tumor cells (5×10^4 cells) were resuspended in PBS (200 μ l) and inoculated subcutaneously into the left mammary gland. The day a palpable tumor could be confirmed was defined as tumor onset day in the Kaplan–Meier plot. (a) Bar graphs represent the gene expression of *Irf7*, *Ifi44*, and *Usp18* in Ctrl, *Irf7* transgenic, *Ifi44* transgenic, and *Usp18* transgenic 4T1A cell lines ($n = 5$). (b) Bar graphs represent the gene expression of *Ifi44* and *Usp18* in Ctrl and *Irf7* transgenic CT26 cell lines ($n = 2$). (c) Western blotting of *Irf7* in 4T1A, 4T1S, and *Irf7*KO 4T1S cell lines with/without radiation. α Tubulin served as an internal positive control. The bands are quantified by ImageJ and shown in red letters. (d) Kaplan–Meier plot of tumor-free and overall survival in BALB/c mice vaccinated with Ctrl ($n = 6$) and *Irf7*KO 4T1S ($n = 8$) cells after radiation. Mice were challenged with 4T1S cells 14 days after the vaccination. Gene expression levels were determined by RT-PCR, as normalized to *Gapdh*. Values were analyzed by a Tukey–Kramer test (a) and a Log-rank test (d) and are shown as mean \pm SEM (a). Asterisk indicates a significant difference; * $P < 0.05$, ** $P < 0.01$, *** $P < 0.001$, compared with the control group.

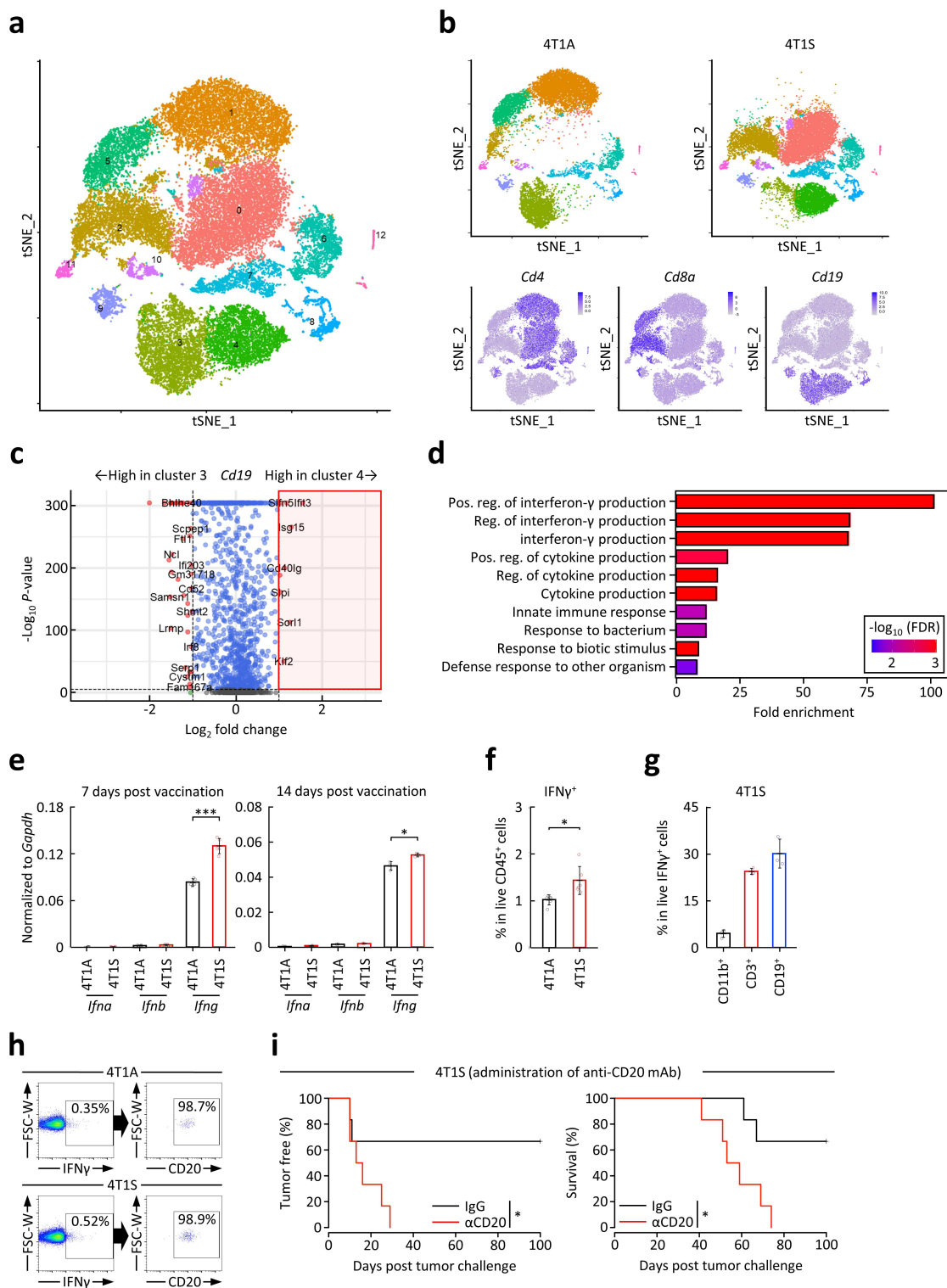


Figure 4. Effects of IFN γ ⁺ B cells on vaccine effectiveness by irradiated whole tumor cells. Lymph nodes of each mouse were collected 14 days after vaccination with 4T1A or 4T1S and prepared as single-cell libraries, then sequenced on the next-generation sequencer. Based on acquired raw sequencing data, gene expression matrices for each cell were generated. The resulting count matrices were further processed using the Seurat to remove low-quality cells. Then, t-distributed stochastic neighbor embedding (tSNE) projections allowed us to assign cells to 12 clusters. Cell types were annotated using the Louvain algorithm based on known cell markers and differential gene expression analysis. Highly expressed genes in *CD4*, *CD8a*, and *CD19* clusters within 4T1S vaccinated murine lymph node cells were identified by mean expression and variance compared to 4T1A vaccinated murine lymph node cells and were visualized using the Volcano plots. For in vivo prophylactic vaccination assay, tumor cells (2×10^6 cells) were resuspended in PBS (200 μ l) and inoculated subcutaneously into the right back of syngeneic female mice after X-rays (300 Gray). Two weeks after vaccination, tumor cells (5×10^4 cells) of the same type as at the time of vaccination were resuspended in PBS (200 μ l) and inoculated subcutaneously into the left mammary gland. Anti-CD20 antibodies (250 μ g) were intraperitoneally administered 7 days before, one day before, and 7 days after vaccination. The day a palpable tumor could be confirmed was defined as tumor onset day in the Kaplan–Meier plot. (a) tSNE projection represent all lymph node cells of both 4T1A and 4T1S vaccinated mice that passed quality control ($n = 36814$ cells). Twelve clusters were defined and indicated by different colors. (b) tSNE projection represents lymph node cells of 4T1A or 4T1S vaccinated mice (4T1A: $n = 16295$ cells, 4T1S: $n = 20519$ cells). The purple color highlights the *Cd4*, *Cd8a*, and *Cd19* clusters. (c) Volcano plots of differentially expressed genes ($P < 0.01$) in *Cd19*⁺ cells of 4T1S vaccinated mice. Black dots symbolize genes not significantly different, and each dot denotes a single gene. The x-axis is the fold change of gene expression (Log_2) in each *Cd19*⁺ cell, and the y-axis represents Log_{10} of the P -value. (d) Gene ontology enrichment analysis of

secondary lymphoid tissue, such as the spleen and lymph nodes, was compared 3, 7, and 14 days after vaccination. Unexpectedly, between 4T1A- and 4T1S-vaccinated mice, no changes in T or B cells, which are predominant fractions in secondary lymphoid tissues, were observed (Figure S3a, b). Other immune cells were also not altered or barely existed (Figure S3a, b). Thus, single-cell RNA-sequencing of lymph node cells was performed 14 days after vaccination (the day of tumor challenge) in 4T1A- and 4T1S-vaccinated mice (Figure 4a). Consequently, noticeable population differences were observed in CD4⁺ T, CD8⁺ T, and CD19⁺ B cell fractions induced by 4T1A or 4T1S vaccination (Figure 4b).

In CD4⁺ T-cell fractions, results of the analysis of differentially expressed genes to explore the difference in the population induced by each vaccine showed that the expressions of 14 genes were significantly increased in CD4⁺ T cells of 4T1S-vaccinated murine lymph nodes compared with those of 4T1A-vaccinated murine lymph nodes, and the gene enrichment analysis represented that they may be involved in immune-related biological processes, such as myeloid cell differentiation and response to cytokines (Figure S4a, b). A similar analysis in CD8⁺ T-cell fractions indicated that the cells within the lymph nodes of 4T1S-vaccinated mice expressed higher levels of seven genes and may be involved in immune-related biological processes, including response to cytokine (Figure S4c, d). These data suggest that T cells in the lymph nodes induced by 4T1S vaccination generate active immune-related responses. Besides, since T cells are generally known as final effector cells against cancer cells in anti-tumor immunity, the involvement of T cells in the efficacy of 4T1S vaccination was investigated using nude mice (BALB/c *nu/nu*) that lack thymus and cannot produce T cells. As a result, there was no vaccine effectiveness of 4T1S in nude mice (Figure S4e), demonstrating that the dynamics of effective WTCVs shown in this paper require at least the contribution of T cells.

We then performed a similar analysis to CD4⁺ and CD8⁺ T cells for CD19⁺ B cell fractions; nine genes, including *Isg15*, were upregulated in the cells within 4T1S-vaccinated murine lymph nodes (Figure 4c). ISG15 has been known as a driver of IFN γ secretion, and patients congenitally lacking ISG15 cannot produce adequate amounts of IFN γ ²³. Indeed, CD19⁺ B cells within 4T1S-vaccinated murine lymph nodes were shown to be potentially related to the positive regulation of IFN γ production (Figure 4d). As a previous study suggested that IFN γ expression derived from cells in secondary lymphoid tissue may be involved in vaccine effectiveness¹⁵, we focused on this alteration. Reverse transcription-polymerase chain reaction of the IFN family in lymph node cells 7 and 14 days after tumor vaccination revealed that not IFN α or IFN β but only IFN γ was expressed in high levels; its expression was higher in 4T1S-

vaccinated than in 4T1A-vaccinated mice (Figure 4e). Consistent with this, an increment of IFN γ ⁺ lymph node cells in 4T1S-vaccinated mice was observed (Figure 4f). To identify which cells secrete IFN γ within the lymph nodes of 4T1S-vaccinated mice, the frequency of each immune cell in IFN γ ⁺ cells was examined, and CD19⁺ B cells were found to be the primary source of IFN γ production (Figure 4g). Furthermore, IFN γ ⁺CD19⁺ B cells also express CD20 (Figure 4h and Figure S5); thus, we investigated the anti-tumor effect of 4T1S vaccination in mice administered with CD20-depleting antibodies (α CD20) to assess their contribution. The administration of α CD20 resulted in 100% tumor onset within 40 days and the eventual death of all individuals; thus, vaccine effectiveness was fully canceled (Figure 4i).

Lastly, when we ascertain if the same phenomenon occurs following vaccination with cancer cells transfected with *Irf7* and its downstream factors, similar results were obtained with *Irf7/Ifi44/Usp18* transgenic 4T1A or CT26 vaccination (Figure S6a – d). In short, IFN γ expression was increased in the lymph node cells of the vaccinated group with transgenic cancer cells (Figure S6a, c), and α CD20 administration aimed to deplete the source of its production eliminated the tumor-suppression efficacy (Figure S6b, d). Taken together, the above observations are indicative of the scenario that, during vaccination, *Irf7* and its downstream factors (*Ifi44* and *Usp18*) within cancer cells act directly or indirectly on B cells to increase B cell-derived IFN γ expression, and these cell populations then exert recurrence-preventive effects cooperated with T cells.

Discussion

This study demonstrated for the first time a novel strategy for converting the characteristics of less immunogenic cancer cells, that is, to increase their immunogenicity, by transfecting *Irf7* and its downstream factors into cancer cells via in vivo vaccination experiments, the gold standard for detecting immunogenic cell death. WTCVs transfected with *Irf7*, *Ifi44*, and *Usp18* dramatically reduced the risk of tumor onset in all cancer types that were challenged, resulting in the prolongation of murine survival. Moreover, its beneficial phenomenon appeared to be mediated by the type II IFN response of B cells.

Irf7, *Ifi44*, and *Usp18* play vital roles in the innate immune response to foreign pathogens in immune cells^{21,22}. Nevertheless, they were also highly expressed in vaccine-effective cancer cells and finally triggered a type II IFN response in B cells. Indeed, only a few studies have focused on innate immune pathways in tumor cells. A previous study regarding such content reported that in experiments using a mouse model, *Irf7* expression in tumor cells, and not in immune cells, suppressed metastasis and prolonged survival

highly expressed genes in *Cd19*⁺ cells of 4T1S vaccinated mice. (e) Bar graphs represent the gene expression of *Ifna*, *Ifnb*, and *Ifng* in lymph node cells of 4T1A or 4T1S vaccinated mice (n = 3-5). Gene expression levels were determined by RT-PCR, as normalized to *Gapdh*. (f) Bar graphs represent the frequency of IFN γ ⁺ cells within CD45⁺ cells in lymph node cells of 4T1A or 4T1S vaccinated mice (n = 5). (g) Bar graphs represent the frequency of CD11b⁺, CD3⁺, and CD19⁺ cells within IFN γ ⁺ cells in lymph node cells of 4T1S vaccinated mice (n = 3). (h) Representative plots of IFN γ ⁺ cells within CD19⁺ cells (left) and CD20⁺ cells gated from them (right) in lymph node cells of 4T1A or 4T1S vaccinated mice. (i) Kaplan–Meier plot of tumor-free and overall survival in BALB/c mice vaccinated with 4T1S cells after radiation and administered with anti-CD20 antibodies (n = 6). Mice were challenged with 4T1S cells 14 days after the vaccination. Values were analyzed by a Tukey–Kramer test (c), a two-sided Student's t-test (e-g), and a Log-rank test (i) and are shown as mean \pm SEM (e-g). Asterisk indicates a significant difference; **P*<0.05, ****P*<0.001, compared with the control group.

by activating the immune system²⁴. Besides, analysis of human clinical data showed that high expression levels of *Irf7*-regulated genes in breast cancer tissues were associated with fewer recurrences to the bone²⁴. Although *Irf7* can regulate whole IFN-inducible pathways, unlike our claim, most of these *Irf7*-derived mechanisms mediate type I IFN pathways, which are potent regulators of most effector cells involved in antiviral immune responses²⁵. Indeed, in the above paper, *Irf7*-deficient mice had accelerated metastasis even if *Irf7* expression was induced in tumor cells, and *Irf7* did not exert suppressive effects²⁴. Moreover, IFN α administration reduced metastasis and prolonged metastasis-free survival²⁴. Accordingly, *Irf7* in tumor cells can induce type I IFN response in immune cells, suppressing metastasis. However, most of these findings address primary tumors, and no prior evidence shows that *Irf7* in WTCVs prevents cancer recurrence.

Irf7 is also involved in type II IFN response in immune cells¹⁶. Specifically, a study revealed that IFN γ production was enhanced in splenocytes from mice immunized with IFN α transgenic tumor cells¹⁵. It has been assumed that IFN γ is mainly produced by T and natural killer (NK) cells²⁶; indeed, *Irf7* can increase the frequency of IFN γ -producing antigen-specific CD8⁺ T cells¹⁶. On the contrary, our data showed the possibility that the *Irf7* axis increases the frequency of IFN γ -producing B cells, suggesting the novel dynamics of anti-tumor immunity derived from *Irf7*.

Accumulating evidence demonstrates the benefit of localized IFN γ secretion to induce potent anti-tumor immunity^{27,28}. The IFN γ -induced immune response initially appears local rather than systemic; however, it finally leads to a tumor-specific long-term memory immunity¹⁴. Among immune cells capable of producing type II IFN, B cells functioning as antigen-presenting cells can initiate Th1 cell activation and IFN γ production²⁹. Contrary to this, Th1 cells can induce B cell activation and their IFN γ production³⁰. IFN γ -producing B cells not only amplify type I immune responses but also imprint a type I phenotype on B cells themselves³⁰. Consequently, IFN γ has been reported to drive the positive feedback loop via B cells in immune responses to bacterial or viral pathogens³⁰. Interestingly, the deletion of the IFN γ receptor in B cells abrogates systemic autoimmunity²⁹. Also in tumor immunity, it has been documented that B cells polarize into IFN γ -producing types under the influence of Th1 cells³¹. Besides, activating B cells by intra-tumoral injection of IL-12 induced immunoglobulin and IFN γ production, leading to good outcomes in head and neck cancer patients³². This suggests that IFN γ -producing B cells have a multifaceted role in anti-tumor immunity and can contribute to both the innate and adaptive immune responses against cancer. Given these contexts, our data that the depletion of IFN γ -producing B cells disrupted the efficacy of WTCVs appears sufficiently convincing.

Despite growing evidence implicating type I and II IFNs as fundamental mediators in various diseases, the potential role of the *Irf7* axis, which is the upstream regulatory factor of IFN pathways in anti-tumor immune responses of WTCVs, has hitherto been fully unknown. This study clarified that introducing *Irf7*, *Ifi44*, and *Usp18*, three factors of the *Irf7* axis, into cancer cells could augment the recurrence-preventive efficacy of WTCVs. In addition, the silencing of *Irf7*, upstream of *Irf7*,

Ifi44, and *Usp18*, in originally vaccine-effective cancer cells resulted in a void of its ability. As the mechanisms that *Irf7* axis enhances vaccine effectiveness, IFN γ -producing not T or NK cells but B cells enhanced anti-tumor immune responses. Because of some unclear points, including how *Irf7* in cancer cells stimulates B cells, followed by increased IFN γ production from B cells, further basic research is required. Advances in research and development of this therapeutic strategy may establish novel therapeutic options to prevent cancer recurrence and allow more patients to benefit from it. Specifically, a possible approach involves isolating cancer cells from surgically removed fresh tumor tissue, followed by the transfection of candidate genes and inactivation by X-ray. Eventually, patients are vaccinated with gene-modified and irradiated autologous cancer cells as WTCVs, which may lead to relapse prevention. Taken together, our findings will prompt future research of recurrence-preventive cancer vaccines targeting the *Irf7* axis in cancer and may apply as a prophylactic treatment in the clinical setting.

Acknowledgments

The authors thank Ms. Rei Okabe, Ms. Nanami Eguchi, Ms. Chie Kusama, and Ms. Ayano Yamauchi for their technical assistance.

Disclosure statement

No potential conflict of interest was reported by the authors.

Funding

This work was partly supported by research grants from the Ministry of Education, Culture, Sports, Science and Technology of Japan (#22K19449, K. Seino, #18K07286, H. Wada), Joint Research Program of the Institute for Genetic Medicine (K. Seino), the project of junior scientist promotion (K. Seino), the Photo-excitonix Project in Hokkaido University (K. Seino), GSK Japan Research Grant 2021 (H. Wada), JST SPRING (#JPMJSP2119, N. Kajihara), and JSPS KAKENHI (#22J21076, N. Kajihara).

ORCID

Haruka Wada  <http://orcid.org/0000-0002-5526-3647>

Author contributions

NK, KS, and HW designed the study. NK, HW, YT, and RT performed experiments. All authors analyzed data and discussed the results. NK, KS, and HW contributed to manuscript preparation. All authors approved the final version of this manuscript for publication.

Data availability statement

The datasets generated and/or analyzed during the current study are available from the corresponding author on reasonable request.

References

1. Sheikhi A, Jafarzadeh A, Kokhaei P, Hojjat-Farsangi M. Whole tumor cell vaccine adjuvants: comparing IL-12 to IL-2 and IL-15. *Iran J Immunol*. 2016;13:148–166.

2. Wang F, Gao J, Wang S, Jiang J, Ye Y, Ou J, Liu S, Peng F, Tu Y. Near infrared light activation of an injectable whole-cell cancer vaccine for cancer immunoprophylaxis and immunotherapy. *Biomater Sci.* 2021;9:3945–3953. doi:10.1039/d1bm00542a.
3. Aikins ME, Xu C, Moon JJ. Engineered nanoparticles for cancer vaccination and immunotherapy. *Acc Chem Res.* 2020;53:2094–2105. doi:10.1021/acs.accounts.0c00456.
4. Lollini PL, Cavallo F, Nanni P, Quaglino E. The promise of preventive cancer vaccines. *Vaccines (Basel).* 2015;3:467–489. doi:10.3390/vaccines3020467.
5. Keenan BP, Jaffee EM. Whole cell vaccines - Past progress and future strategies. *Semin Oncol.* 2012;39:276–286. doi:10.1053/j.seminoncol.2012.02.007.
6. Liu J, Fu M, Wang M, Wan D, Wei Y, Wei X. Cancer vaccines as promising immuno-therapeutics: platforms and current progress. *J Hematol Oncol.* 2022 15; 15: doi:10.1186/s13045-022-01247-x.
7. Huber ML, Haynes L, Parker C, Iversen P. Interdisciplinary critique of sipuleucel-T as immunotherapy in castration-resistant prostate cancer. *J Natl Cancer Inst.* 2012;104:273–279. doi:10.1093/jnci/djr514.
8. Joshi VB, Geary SM, Gross BP, Wongrakpanich A, Norian LA, Salem AK. Tumor lysate-loaded biodegradable microparticles as cancer vaccines. *Expert Rev Vaccines.* 2014;13:9–15. doi:10.1586/14760584.2014.851606.
9. Al-Tameemi M, Chaplain M, D'onofrio A. Evasion of tumours from the control of the immune system: consequences of brief encounters. 2012; 7: 31. <http://www.biology-direct.com/content/7/1/31>.
10. Au KM, Balhorn R, Balhorn MC, Park SI, Wang AZ. High-performance concurrent chemo-immuno-radiotherapy for the treatment of hematologic cancer through selective high-affinity ligand antibody mimic-functionalized doxorubicin-encapsulated nanoparticles. *ACS Cent Sci.* 2019;5:122–144. doi:10.1021/acscentsci.8b00746.
11. Abe H, Wada H, Baghdadi M, Nakanishi S, Usui Y, Tsuchikawa T, Shichinohe T, Hirano S, Seino KI. Identification of a highly immunogenic mouse breast cancer sub cell line, 4t1-s. 2016;29:58–66. 10.1007/s13577-015-0127-1. *Hum Cell.*
12. Soiffer RJ, Kooshesh KA, Ho V. Whole tumor cell vaccines engineered to secrete GM-CSF (GVAX). *ImmunoMedicine.* 2021;1. doi:10.1002/imed.1025.
13. Hege KM, Jooss K, Pardoll D. GM-CSF gene-modified cancer cell immunotherapies: of mice and men. *Int Rev Immunol.* 2006;25:321–352. doi:10.1080/08830180600992498.
14. Gansbacher B, Bannerji R, Daniels B, Zier K, Cronin K, Gilboa E. Retroviral vector-mediated gamma-interferon gene transfer into tumor cells generates potent and long lasting antitumor immunity. 1990; 50: 7820–7825. <http://aacrjournals.org/cancerres/article-pdf/50/24/7820/2442042/cr0500247820.pdf>.
15. Omori R, Eguchi J, Hiroishi K, Ishii S, Hiraide A, Sakaki M, Doi H, Kajiwara A, Ito T, Kogo M, et al. Effects of interferon- α -transduced tumor cell vaccines and blockade of programmed cell death-1 on the growth of established tumors. *Cancer Gene Ther.* 2012;19:637–643. doi:10.1038/cgt.2012.42.
16. Castaldello A, Sgarbanti M, Marsili G, Brocca-Cofano E, Remoli AL, Caputo A, Battistini A. Interferon regulatory factor-1 acts as a powerful adjuvant in tat DNA based vaccination. *J Cell Physiol.* 2010;224:702–709. doi:10.1002/jcp.22169.
17. Kepp O, Tartour E, Vitale I, Vacchelli E, Adjemian S, Agostinis P, Apetoh L, Aranda F, Barnaba V, Bloy N, et al. Consensus guidelines for the detection of immunogenic cell death. *Oncoimmunology.* 2014;3:e955691. doi:10.4161/21624011.2014.955691.
18. Golden EB, Apetoh L. Radiotherapy and immunogenic cell death. *Semin Radiat Oncol.* 2015;25:11–17. doi:10.1016/j.semradonc.2014.07.005.
19. Perez CA, Fu A, Onishko H, Hallahan DE, Geng L. Radiation induces an antitumour immune response to mouse melanoma. *Int J Radiat Biol.* 2009;85:1126–1136. doi:10.3109/09553000903242099.
20. Muragaki Y, Maruyama T, Iseki H, Tanaka M, Shinohara C, Takakura K, Tsuboi K, Yamamoto T, Matsumura A, Matsutani M, et al. Phase I/IIa trial of autologous formalin-fixed tumor vaccine concomitant with fractionated radiotherapy for newly diagnosed glioblastoma - Clinical article. *J Neurosurg.* 2011;115:248–255. doi:10.3171/2011.4.JNS10377.
21. McDonald JU, Kaforou M, Clare S, Hale C, Ivanova M, Huntley D, Dorner M, Wright VJ, Levin M, Martinon-Torres F, et al. A simple screening approach to prioritize genes for functional analysis identifies a role for interferon regulatory factor 7 in the control of respiratory syncytial virus disease. *mSystems.* 2016 1: 10.1128/msystems.00051-16.
22. Coit P, Ortiz-Fernandez L, Lewis EE, McCune WJ, Maksimowicz-McKinnon K, Sawalha AH. A longitudinal and transancestral analysis of DNA methylation patterns and disease activity in lupus patients. *JCI Insight.* 2020 5; 5: 10.1172/jci.insight.143654.
23. Bogunovic D, Byun M, Durfee LA, Abhyankar A, Sanal O, Mansouri D, Salem S, Radovanovic I, Grant AV, Adimi P, et al. Mycobacterial disease and impaired IFN- γ immunity in humans with inherited ISG15 deficiency. *Science (1979).* 2012;337:1684–1688. doi:10.1126/science.1224026.
24. Bidwell BN, Slaney CY, Withana NP, Forster S, Cao Y, Loi S, Andrews D, Mikeska T, Mangan NE, Samarajiwa SA, et al. Silencing of Irf7 pathways in breast cancer cells promotes bone metastasis through immune escape. *Nat Med.* 2012;18:1224–1231. doi:10.1038/nm.2830.
25. Ning S, Pagano JS, Barber GN. IRF7: activation, regulation, modification and function. *Genes Immun.* 2011;12:399–414. doi:10.1038/gene.2011.21.
26. Aldridge DL, Phan AT, de Waal Malefyt R, Hunter CA. Limited Impact of the inhibitory receptor TIGIT on NK and T cell responses during toxoplasma gondii infection. *Immunohorizons.* 2021;5:384–394. doi:10.4049/immunohorizons.2100007.
27. Abdel-Wahab Z, Dar MM, Hester D, Vervaert C, Gangavalli R, Barber J, Darrow TL, Seigler HF. Effect of irradiation on cytokine production, MHC antigen expression, and vaccine potential of interleukin-2 and interferon-gamma gene-modified melanoma cells. 1996;171:246–254. doi:10.1006/cimm.1996.0200.
28. Abdel-Wahab Z, Weltz C, Hester D, Pickett N, Vervaert C, Barber JR, Jolly D, Seigler HF. A phase I clinical trial of immunotherapy with interferon- γ gene-modified autologous melanoma cells: monitoring the humoral immune response. *Cancer.* 1997;80:401–412. doi:10.1002/(SICI)1097-0142(19970801)80:3<401:AID-CNCR8>3.0.CO;2-U.
29. Jackson SW, Jacobs HM, Arkatkar T, Dam EM, Scharping NE, Kolhatkar NS, Hou B, Buckner JH, Rawlings DJ. B cell IFN- γ receptor signaling promotes autoimmune germinal centers via cell-intrinsic induction of BCL-6. *J Exp Med.* 2016;213:733–750. doi:10.1084/jem.20151724.
30. Harris DP, Goodrich S, Gerth AJ, Peng SL, Lund FE. Regulation of IFN- γ production by B effector 1 cells: essential roles for T-bet and the IFN- γ receptor. *J Immunol.* 2005;174:6781–6790. doi:10.4049/jimmunol.174.11.6781.
31. Guo FF, Cui JW. The role of tumor-infiltrating B cells in tumor immunity. *J Oncol.* 2019;2019:1–9. doi:10.1155/2019/2592419.
32. Van Herpen CML, Van Der Voort R, JAWM VDL, Klasen IS, De GA, Van Kempen LCL, De Vries IJM, Duiveman-De BT, Dolstra H, Torensma R, et al. Intratumoral rhIL-12 administration in head and neck squamous cell carcinoma patients induces B cell activation. *Int J Cancer.* 2008;123:2354–2361. doi:10.1002/ijc.23756.